

**Final Report on Grant NAG5-5086  
Ion Mass Spectrometer for Sporadic-E Rocket Experiments**

Table of Contents

1. Introduction
  - A. Experiment Overview
  - B. The Role of the William B. Hanson Center for Space Sciences
  - C. Logistics
2. Instrument Design
  - A. Mechanical Design & Specifications
  - B. Electrical Design & Specifications
3. In-Flight Performance and Science Data
  - A. Payload 21.115
  - B. Payload 21.116
4. Publications and Conference Presentations
5. Conclusion
6. Appendix - Reprint of a paper published in *Geophysical Research Letters*

## **INTRODUCTION**

NASA grant NAG5-5086 provided funding for the William B. Hanson Center for Space Sciences at the University of Texas at Dallas (UTD) to design, fabricate, calibrate, and ultimately fly two ion mass spectrometer instruments on a pair of sounding rocket payloads. Drs. R.A. Heelis and G.D. Earle from UTD were co-investigators on the project. The principal investigator for both rocket experiments was Dr. Robert Pfaff of the Goddard Space Flight Center. The overall project title was "Rocket/Radar Investigation of Lower Ionospheric Electrodynamics Associated with Intense Mid-Latitude Sporadic-E Layers". This report describes the overall objectives of the project, summarizes the instrument design and flight experiment details, and presents representative data obtained during the flights.

### **Experiment overview**

The experiment plan proposed by Dr. Pfaff called for flying a total of four sounding rockets in two salvos of two rockets each. Each salvo was to consist of one heavily instrumented sounding rocket equipped to measure electric fields, ion composition, neutral pressure variations, and magnetic fields. The second rocket in each salvo was intended to be launched within minutes of the instrumented rocket. Its function was to release trimethyl-aluminum (TMA), a chemiluminescent material that reacts strongly with oxygen to produce a glowing gas cloud that is visible from the ground. The plan was to observe the drift of these gas clouds from ground-based sites, and to use these data to infer the neutral winds throughout the lower E region of the ionosphere. These neutral wind data could then be compared with the *in-situ* measurements from the instrumented rockets, as well as with radar data obtained simultaneously from a coherent scatter radar system provided by the University of Illinois.

### **The Role of the William B. Hanson Center for Space Sciences**

UTD's role was to supply the ion mass spectrometers for the two instrumented rockets, to analyze the resulting data, and to work with scientists from other institutions to assimilate the results. This work has been completed, but as with any complex experiment, efforts will continue for some time in order to fully understand the significance of the results. Supplying the instruments for the rocket flights involved many steps, including basic instrument design, fabrication, laboratory-based testing and calibration, integration onto the rocket payload, environmental testing, field transport and check-out, and participation in launch-related activities.

### **Logistics**

The initial experiment plan called for all four rocket launches to occur from Tortuguero, Puerto Rico as part of the El Coqui Dos sounding rocket campaign. This campaign included 11 rockets and relied heavily on scientific support from the Arecibo incoherent scatter radar facility, the most powerful radio telescope in the world. Unfortunately for the campaign, political unrest in Puerto Rico resulted in difficulties at the rocket range that ultimately affected the experiments with which UTD was involved. Specifically, of the four rocket launches planned as part of our experiment only one was successfully carried out; the first instrumented launch. The second instrumented payload and both TMA payloads were eventually launched from Wallops Island, Virginia over a year later. Despite these logistical problems this report will show that the instruments provided by UTD functioned exceptionally well, and yielded new results regarding

plasma layering processes and neutral winds in the dynamic region of space between 90 and 115 km in altitude.

## INSTRUMENT DESIGN

The mass spectrometers designed under grant NAG5-5086 were identified by the acronym PRIMS, for Puerto Rico Ion Mass Spectrometer. The two instruments were built to exactly the same design specifications, and were capable of directly measuring the concentration of four distinct ion species known to be the major constituents of the lower thermosphere. Specifically, these four ions of interest were  $\text{NO}^+$ ,  $\text{O}_2^+$ ,  $\text{Mg}^+$ , and  $\text{Fe}^+$ . The first two are molecular ions formed from the ambient atmospheric gas by photo-ionization, and the latter are metallic ions that are formed by meteor ablation in the upper atmosphere. The masses of the ions of interest are respectively 30, 32, 24, and 56 amu. The objective of the PRIMS instruments was to unambiguously measure the concentration of all four species in order to allow comparisons with simultaneously measured electric fields, magnetic fields, and neutral winds.

### Mechanical Design & Specifications

Figure 1 shows the flight configuration outline for the PRIMS instruments. The overall instrument can be thought of as consisting of four distinct modules:

1. Aperture cover assembly;
2. Getter pump and ion-pump systems;
3. Analyzer compartment;
4. Electronics.

The PRIMS instrument was intended for use at altitudes above about 100 km, where the atmospheric pressure is less than 0.1 millitorr. In order to function correctly at these altitudes within a few minutes of launch it is necessary to maintain a good vacuum inside the instrument during countdown and testing procedures. This was accomplished using a vacuum tight breakable glass seal around the instrument's aperture. UTD therefore designed and tested a break-seal system that prevented high pressure atmospheric gas from leaking into the device prior to it reaching the desired altitude. The seal was broken at a pre-specified time in the flight by activation of a non-outgassing squib assembly, as shown in Figure 1.

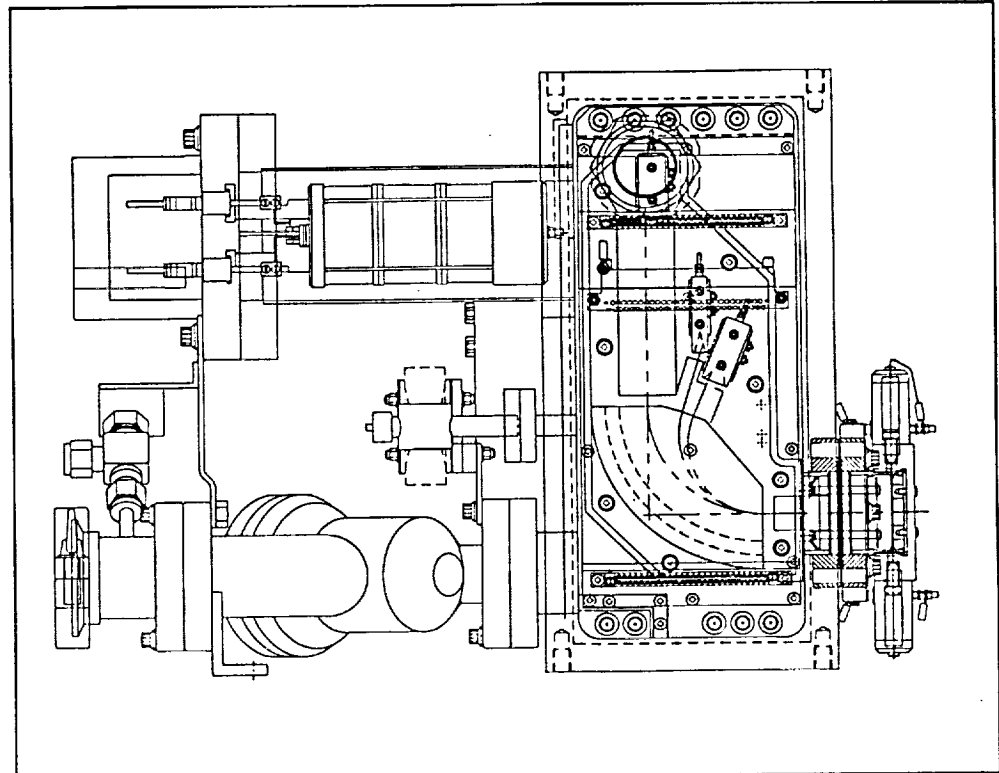
The getter pump and ion-pump systems were used to maintain and to verify the presence of vacuum levels below  $10^{-4}$  Torr during testing and integration. In so doing these systems ensured the cleanliness of the analyzer compartment (*i.e.*, absence of water vapor and other contaminants) and provided confidence in their ability to function correctly when turned on at altitude. The getter pump housing, ion-pump/gauge, and flanges for an external pump used in field support operations are all shown in Figure 1.

Figure 2 shows a view of the analyzer compartment within the instrument. The aperture is located on the bottom right in the figure, and the analyzer compartment is the rectangular section immediately left of the entrance aperture (and deployable cover, as shown). The quadrant immediately inside the aperture is a 4 kG sector magnet whose function is to separate the incoming ions by imparting different radial trajectories according to their masses. This magnetic separation follows the relationship:

$$R^2 = \frac{2mKT}{e^2B^2}$$



where  $R$  is the radius of the ion orbit,  $m$  is the ion mass,  $K$  is Boltzmann's constant,  $T$  is the ion temperature,  $e$  is the fundamental unit of electronic charge, and  $B$  is the magnetic field strength. All of the above quantities are in mks units. Our analyzer compartment also included an electrostatic deflection system that allowed the same channel electron multiplier (CEM) to measure  $\text{NO}^+$  and  $\text{O}_2^+$  (not simultaneously). By periodically changing this deflector voltage throughout the flight we were able to measure both molecular species without compromising the measurements of the two metallic ions.



**Figure 2** - A detailed view of the entrance aperture, analyzer, and pump systems comprising the PRIMS instrument.

Figure 3 shows the accommodation drawing for the PRIMS instruments within a 17-inch diameter rocket skin section. The instrument utilizes the entire diameter and includes two door sections. One door covers the aperture of the instrument; it is deployed by a separate set of squib circuits prior to breaking the glass cover and opening the instrument's aperture. The second door is diametrically opposite the aperture and allows access to the pump systems. This access port is necessary for connecting the external field vacuum system, and for providing access to the getter and ion-pump systems during testing and integration.

The finished PRIMS instrument is a large and heavy design. Its size makes it suitable for flight on Black-Brant type payloads, or other bulbous payload designs with minimum diameters of 17 inches. The mass of the PRIMS instrument in flight configuration is approximately 52 pounds (23.6 kg). This is largely driven by the stainless steel construction materials used throughout to ensure system cleanliness and vacuum integrity. The design has deliberately not been optimized for weight, in part because the lift capability of Black-Brant type vehicles is more than adequate to reach the altitudes of interest (ballast weights must often be flown to limit apogee to the desirable range).



### Electrical Design & Specifications

Figure 4 shows a functional block diagram of the PRIMS electrical design. High voltage is required to provide electrostatic deflection and to operate the three channel electron multipliers corresponding to the three distinct mass channels. High voltage is turned on via a timed event in flight to minimize the risk of arcing (and consequent damage) in pressure regimes where discharge is likely. By maintaining good vacuum conditions within the instrument at all times, and by turning on the high voltage at a sufficiently high altitude, the risk of damage due to arcing is greatly reduced.

The getter pump system must be initiated by heating, which is accomplished by passing a current of several amps through a resistive medium for a period of several minutes. Subsequent to this heating cycle the getter pump continually operates in flight to maintain a pressure within the analyzer compartment that is less than the ambient pressure. The electronics required to initiate this getter system is a fundamental part of the electrical system design shown in Figure 4. On-board electronics also control the cover deployment mechanism and various system status thermocouple sensors, as shown in the figure.

In addition to the subsystems for analyzer control, status monitors, and getter activation the electronics of the PRIMS instrument includes analyzer high voltage control and pulse counting and telemetry interface circuitry. The analyzer high voltage selects which of the two molecular ion species is currently being measured by the CEM device, as described earlier. The pulse counting circuitry interprets the output of the three separate CEM devices and generates a 10-bit word representing the count rate associated with each mass channel. The data are then passed to the telemetry system via a contiguous 30-bit serial data word.

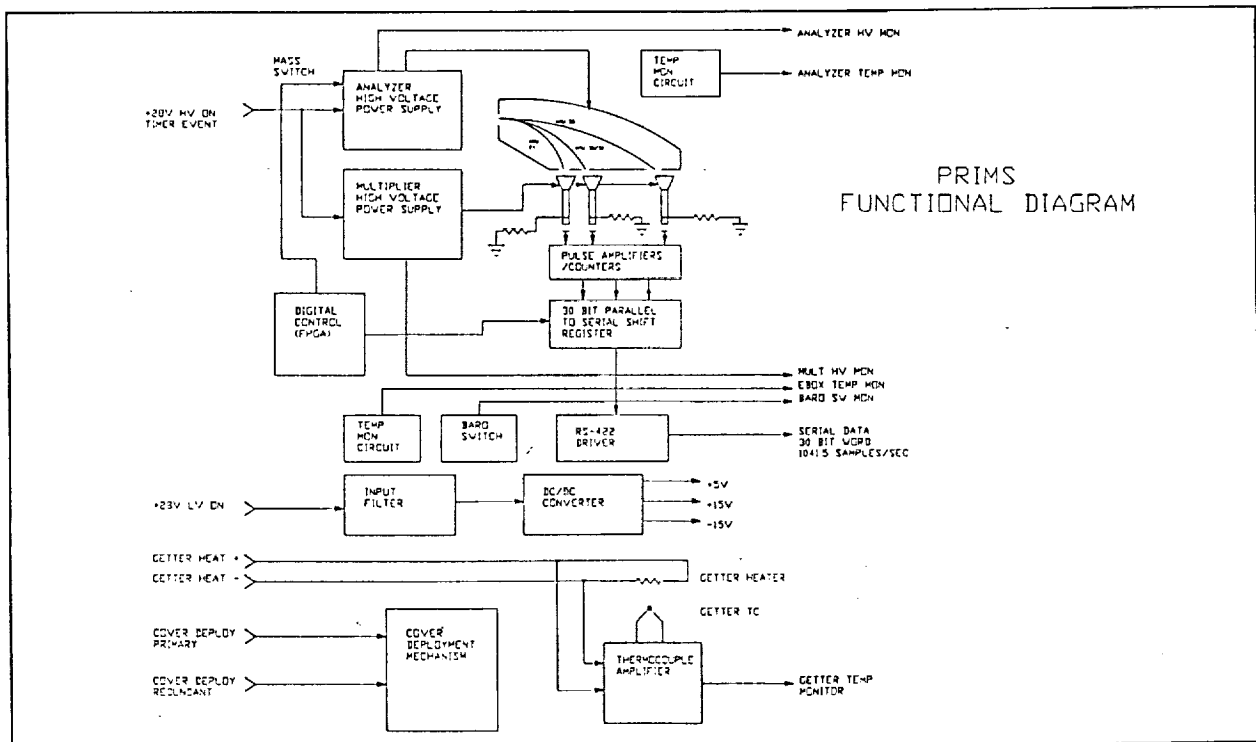


Figure 4 - Functional block diagram of the PRIMS electronics.

**IN-FLIGHT PERFORMANCE AND SCIENCE DATA**

**Payload 21.115**

Sounding rocket 21.115 was successfully launched from Tortuguero, Puerto Rico on the night of 24 March 1998. It carried aloft the first of the two PRIMS instruments as well as other *in-situ* instrumentation for plasma and neutral measurements. As mentioned previously, the second rocket that was intended for near simultaneous launch was not flown during the Puerto Rico campaign. Despite this setback the flight of 21.115 was highly successful, yielding ion composition data that validated a theoretical prediction made in 1969 but never verified experimentally.

Figure 5 shows the data from the PRIMS instrument. The three separate curves shown in the figure correspond to the two metallic ion channels and the combined molecular ion channel. The density of the two molecular species are similar and have been shown combined to maintain clarity in the figure. The sum of the ion content in all three curve traces defines the total ion density in the sporadic-E layer under investigation. The separate ion species that comprise the overall layer are divided into sublayers that are not all centered at the same altitude. This separation of ions based on their respective collision frequencies was predicted over thirty years ago by Chimonas [*J. Geophys. Res.*, 74, 4189, 1969], but had never been observed. This separation, and the structure of the horizontal winds inferred from it, is the subject of a recent paper in *Geophysical Research Letters*, which is included in this report as an appendix.

**Payload 21.116**

The second rocket containing the UTD ion mass spectrometer was launched on 4 July 1999 from the Wallops flight facility. Figure 6 shows the data from this flight. The large depletion in the middle of the sporadic-E layer is caused by spin modulation. Since the mass spectrometer aperture was mounted so as to point out the side of the payload, it was in

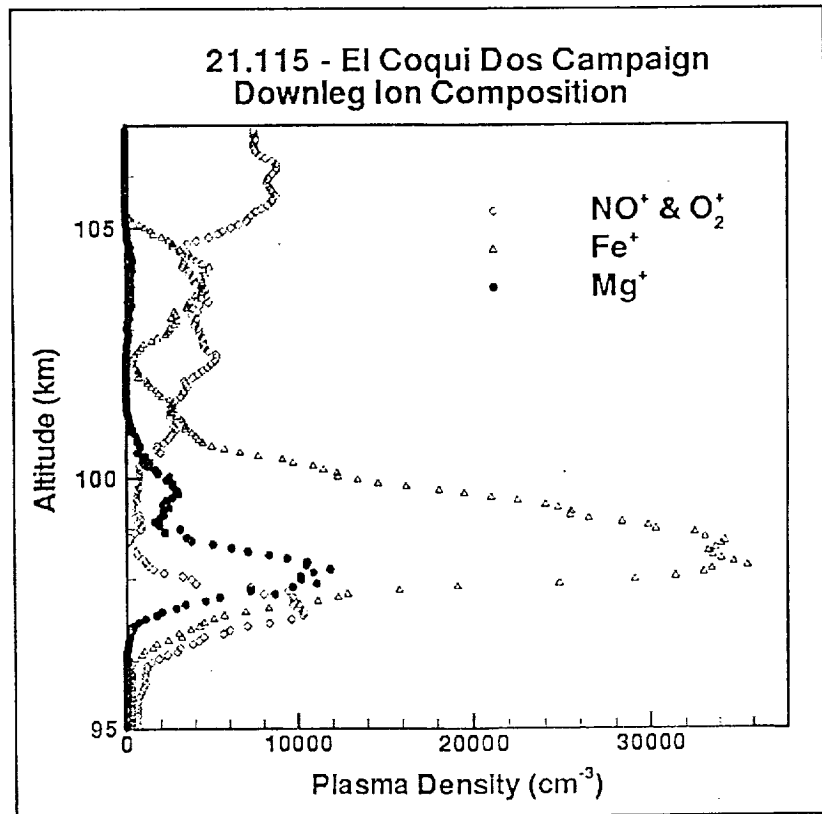


**Figure 5** - Ion mass spectrometer data from the UTD PRIMS instrument. Note the separation of distinct ion sublayers within the sporadic-E layer.

the wake of the payload for roughly half of each spin cycle. This wake effect caused an artificial depletion in the density readings which we are in the process of correcting. Once this artifact is removed from the data we will publish the results in conjunction with data from the other instrumentation aboard the rocket, most notably the neutral wind data (from the TMA rocket) and the *in-situ* electric field measurements.

A comparison of figures 5 and 6 shows that the two sporadic E-layers encountered on the two rocket flights were quite different. The peak density of the layer in the second flight (21.116) was over twice as large as on the first flight, and it does not show any evidence of ion separation into distinct sublayers. Work is ongoing to explain these differences, but it is likely that the lifetime of the layer and the magnitude of the horizontal neutral wind field are responsible for the distinct differences noted. Fortunately wind data from the TMA rocket are available for comparison with the data shown in Figure 6.

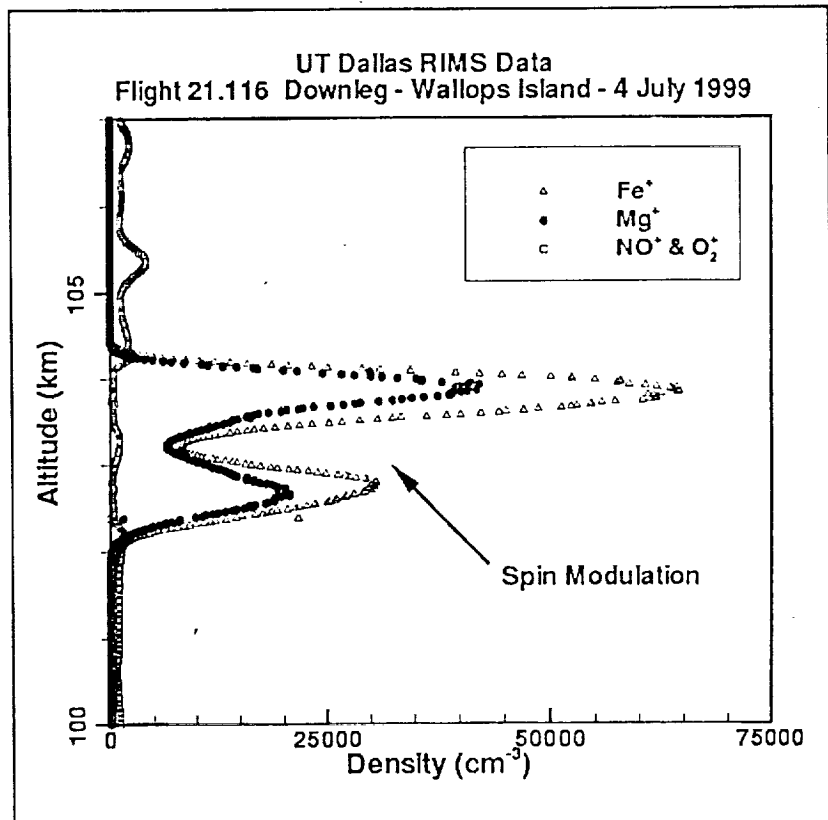


**Figure 6** - Mass spectrometer data from the Wallops Island launch, showing a very intense sporadic-E layer with no vertical separation of ion species.

### PUBLICATIONS AND CONFERENCE PRESENTATIONS

Data from flight 21.115 have already been published. A reprint of the paper is included as an appendix to this document. In addition to this publication, results from both the Puerto Rico and Wallops experiments have been presented and discussed at a variety of conferences, including:

1. Pfaff *et al.*, 1999 Spring Meeting of the American Geophysical Union, Baltimore, MD.
2. Earle *et al.*, 1999 NSF CEDAR Workshop, Boulder, CO.
3. Pfaff *et al.*, 2000 International Symposium on Equatorial Aeronomy, Antalya, Turkey.

In addition to the above presentations, the comprehensive data set from the Wallops Island launches are currently in preparation for publication in the *Journal of Geophysical Research*.

## **CONCLUSION**

The mass spectrometer instruments designed and built by UTD's Hanson Center for Space Sciences have been flown successfully on two different experiments. The design of this complex instrument has been validated through these flights, and the instrument has proven its utility in addressing fundamental scientific questions. The instrument has already been approved for flight on a new rocket mission to be launched in early 2002, and it is a proposed instrument on another new mission to be performed at high latitudes (proposed in response to the ROSS-2000 NRA).

Data quality from the instrument is excellent, and no significant problems have been encountered to date with payload integration, environmental testing, or post-flight data analysis. The UTD mass spectrometer is therefore a viable instrument for future rocket experiments conducted by NASA, and has already gained a solid reputation among the experimental space science community for reliability and data quality. We at the Hanson Center for Space Sciences look forward to many more flight opportunities in the years to come.

**APPENDIX - Reprint of a paper published in *Geophysical Research Letters***

# Ion layer separation and equilibrium zonal winds in midlatitude sporadic E

G.D. Earle

W.B. Hanson Center for Space Sciences, The University of Texas at Dallas, Richardson, Texas

T.J. Kane

Penn State University, State College, Pennsylvania

R.F. Pfaff and S.R. Bounds

NASA Goddard Space Flight Center, Greenbelt, Maryland

**Abstract.** *In-situ* observations of a moderately strong midlatitude sporadic-E layer show a separation in altitude between distinct sublayers composed of Fe<sup>+</sup>, Mg<sup>+</sup>, and NO<sup>+</sup>. From these observations it is possible to estimate the zonal wind field consistent with diffusive equilibrium near the altitude of the layer. The amplitude of the zonal wind necessary to sustain the layer against diffusive effects is less than 10 m/s, and the vertical wavelength is less than 10 km.

## Introduction

Rocket flights through sporadic-E layers have been carried out many times over the last 40 years, with various instrumentation aboard to measure plasma density, electric fields, ion composition, and other parameters [e.g., Seddon, 1962; Smith and Mechty, 1972; Larsen et al., 1998]. During the 1998 El Coqui Dos rocket campaign NASA carried out an experiment that provided high resolution data within a sporadic-E layer [Pfaff et al., 1998]. The experiment plan was to fly two rockets simultaneously, one instrumented to make high quality plasma measurements and another to release trimethyl aluminum (TMA), a pyrophoric material that reacts strongly with oxygen and creates a visible vapor trail. In principle the horizontal neutral wind field can be determined from ground-based optical observations of the TMA trail [Larsen et al., 1998].

Unfortunately, extraneous conditions at the rocket range prevented the launch of the TMA rocket, so no direct neutral wind measurements are available for comparison with the *in-situ* data. Despite this problem, data from the instrumented payload show some very interesting characteristics, including distinct sublayers of metallic ions within the sporadic-E layer. In this paper we present the ion composition measurements from the rocket experiment and compare them to a prediction made by Chimonas [1969] regarding the formation of ion sublayers. In addition, we use a fluid theory description of vertical ion motions in the lower E-region to infer the diffusive equilibrium zonal wind at the altitude of the sporadic-E layer.

## Ion Drift Equations

The physics of the sporadic-E layer formation process was first described by Whitehead [1961] and then independently by

Axford [1963]. The fundamental equation governing ion motion is

$$V_z = \alpha U_E + \beta U_N + \gamma (U_z - g/v_i - \frac{D}{N} \frac{\partial N}{\partial z}) \quad (1)$$

where  $V_z$  is the vertical (positive upward) ion drift, and  $U_E$ ,  $U_N$ , and  $U_z$  are the eastward, northward, and vertical neutral wind components, respectively. In this equation  $v_i$  is the ion-neutral collision frequency,  $g$  is the gravitational acceleration,  $N$  is the ion density, and  $D = KT/mv_i$  is the classical diffusion coefficient. In the calculations that follow we use a temperature of 175 K along with the appropriate mass and collision frequency for each ion species in calculating the diffusion coefficient. The temperature is an average taken from the MSISE-90 standard atmosphere model over the altitude range of interest.

The terms  $\alpha$ ,  $\beta$ , and  $\gamma$  in equation 1 are dimensionless coupling coefficients that relate the net ion motion to the neutral wind vector. They are given by:

$$\alpha = \frac{XZ + R_i Y}{1 + R_i^2} \quad (2)$$

$$\beta = \frac{ZY - XR_i}{1 + R_i^2} \quad (3)$$

$$\gamma = \frac{Z^2 + R_i^2}{1 + R_i^2} \quad (4)$$

where  $X$ ,  $Y$ , and  $Z$  are respectively the direction cosines for the eastward, northward, and upward magnetic field, and  $R_i = v_i/\Omega_i$ , where  $\Omega_i$  is the ion cyclotron frequency.

The general behavior of these coupling coefficients as a function of altitude is similar at all mid-latitude sites, but the magnitudes change somewhat due to different B-field geometries. The zonal wind is much more efficient at producing vertical ion motion than the meridional wind in the lower E-region, although this situation is reversed above about 130 km [Earle et al., 1998]. At altitudes less than about 95 km the zonal and meridional coupling coefficients are both quite small and the vertical transport of ionization is expected to be controlled almost exclusively by the terms multiplied by  $\gamma$  in equation 1.

Equations 1-4 apply separately for each ion species. Chimonas [1969] pointed out that the  $R_i$  term in equations 2-4 is strongly dependent on both the mass and the size of the ion. In

Copyright 2000 by the American Geophysical Union.

Paper number 1999GL900572.  
0094-8276/00/1999GL900572\$05.00

interpreted in many different ways. For example, it could represent an upper bound estimate on the vertical neutral wind, or the vertical phase velocity of a gravity wave. Alternatively, the drift could represent the downward motion of horizontal wind shear, or a sloped sporadic-E layer slowly advecting through the radar beam. The observed downward drift of the layer could also be caused by a small westward electric field, such as the field one would expect at this latitude after sunset. Our data do not preclude any of these interpretations, although it is interesting to note that previous studies using large scale models of the wind field have shown downward drifts of convergent wind shears over time [Wilkinson *et al.*, 1992; Earle *et al.*, 1998].

For altitudes between 95 and 100 km the magnitude of the  $\beta$  term in equation 1 is  $\sim 0.002$ , and  $\alpha$  is about six times larger. The zonal wind is therefore much more effective than the meridional wind in forming layers in the lower E-region, as discussed in the original theoretical treatments by Whitehead [1961] and Axford [1963]. We can estimate the velocity of the zonal wind as a function of altitude using equation 1 in conjunction with the measurements of ion composition and plasma density within the layer. We perform this calculation twice, once using the measured  $\text{Fe}^+$  profile and again using the  $\text{Mg}^+$  profile. The result provides a consistency check on the assumptions and approximations described above. In principle we could repeat the procedure using the  $\text{NO}^+$  profile as well, but the non-negligible recombination effects for molecular ions introduce a time variation into the equations. A time sequence of composition measurements would therefore be required to carry out the calculation self consistently. The rocket observation provides only a snapshot as it passes through the layer, so we have not attempted to do the calculation for the molecular species.

Rearranging equation 1 and neglecting the northward and vertical wind for the reasons discussed above leads to the following expression for the eastward wind near the layer

$$U_E = \frac{1}{\alpha} \left( V_z + \frac{\gamma g}{v_i} - \frac{\gamma D}{N} \frac{\partial N}{\partial z} \right). \quad (5)$$

There are two possible approaches to using the above equation to estimate the zonal wind. If one assumes that the apparent downward motion of the sporadic-E layer represents an actual vertical ion drift caused solely by the zonal wind, then  $V_z = -2$  m/s should be substituted into equation 5 along with the appropriate values for the other variables. The last two terms on the right side of equation 5 are then negligible relative to the  $V_z$  term, and the wind evaluates to roughly 160 m/s in the westward direction over the entire altitude range from 95-105 km.

We consider this approach to be questionable for several reasons. First, if such large winds were common at the altitude of sporadic-E there would be clear signatures in both ground-based and satellite-based airglow measurements, and no such observations have been reported. Second, this approach leads to a very large westward wind that overwhelms the shear in the wind profile, in contrast to the basic mechanism for sporadic-E formation described by Whitehead [1961] and Axford [1963]. Although Larsen *et al.* [1998] have measured very large winds near a sporadic-E layer, their wind measurements contained a large shear that was ostensibly the source of the layer. Finally, many alternative explanations for the apparent downward drift of the layer are more feasible, as discussed below.

A more likely scenario in our view is that the large scale downward motion of the layer is caused by the gradual descent of a convergent node in the wind profile, or by a small westward electric field. Since the radar data were obtained at vertical

incidence, it is also possible that the apparent descent of the layer is caused by the tilted phase front of a gravity wave advecting through the radar beam. In either case the profile of the layer would be maintained by a wind shear and could be treated as a separate effect. To analyze this case we set  $V_z = 0$  and solve for the zonal wind field necessary to maintain the layer shape against diffusion. Figure 3 shows the resultant zonal wind field obtained using the measured ion density profiles. The solid line shows the result of the calculation using the  $\text{Fe}^+$  profile, and the dotted line shows the result for the  $\text{Mg}^+$  profile. The wind profile derived from the  $\text{Mg}^+$  data is broken into two segments, since the calculation is not viable when the density of the ion species is too small. We have somewhat arbitrarily chosen a density of  $30 \text{ cm}^{-3}$  as the cut-off for obtaining a reliable wind estimate.

## Discussion

Although the calculations involved in obtaining the wind profiles shown in Figure 3 were carried out independently for the two ion species, the inferred equilibrium winds have very similar trends. The fact that these winds are in good agreement when the metallic ion peaks for  $\text{Mg}^+$  and  $\text{Fe}^+$  are separated in altitude supports Chimonas' [1969] conjecture that differences in the  $R_i$  parameter in equations 2-4 produce ion sublayers. We interpret this as additional evidence that the assumptions and approximations invoked in our analysis are reasonable.

Some interesting conclusions can be drawn from the zonal wind data presented in Figure 3. First, the result suggests that large zonal wind shears are not necessary to maintain high density sporadic-E layers. The layer near 98 km altitude is by far the most dense encountered by the rocket, yet the derived wind shear is quite weak ( $\Delta U/\Delta z \sim 0.003 \text{ s}^{-1}$ ). The diffusive equilibrium wind amplitudes and shear strengths we infer from our data are very different from those measured in a study by Larsen *et al.* [1998] using TMA vapor trail measurements near a sporadic E-layer that was highly unstable. They calculated Richardson numbers less than 0.25, indicative of unstable flows. The layer described in this paper is less dynamic, and the

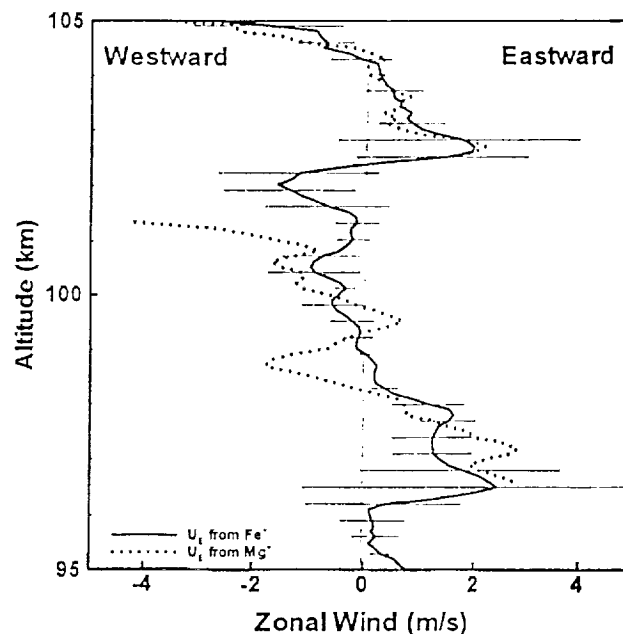


Figure 3. Diffusive equilibrium zonal wind profile derived from ion composition data using equations 1-4.